arXiv:1702.04540v1 [math.NA] 15 Feb 2017

DISPERSION OPTIMIZED QUADRATURES FOR ISOGEOMETRIC ANALYSIS

VICTOR CALO*, QUANLING DENG†, AND VLADIMIR PUZYREV‡

Abstract. We develop and analyze quadrature blending schemes that minimize the dispersion error of isogeometric analysis up to polynomial order seven with maximum continuity in the span (C^{p-1}). The schemes yield two extra orders of convergence (superconvergence) on the eigenvalue errors, while the eigenfunction errors are of optimal convergence order. Both dispersion and spectrum analysis are unified in the form of a Taylor expansion for eigenvalue errors. As a consequence, the schemes increase the accuracy and robustness of isogeometric analysis for wave propagation as well as the differential eigenvalue problems. We analyze the methods' robustness and efficacy and utilize numerical examples to verify our analysis of the performance of the proposed schemes.

AMS subject classifications. 65N15, 65N30, 65N35, 35J05

Key words. isogeometric analysis, quadrature rule, dispersion analysis, spectrum analysis

1. Introduction.

Isogeometric analysis is a widely-used numerical method introduced by Hughes and his collaborators [13, 21] in 2005. Approximation, stability, and error estimates are established in [7]. Structural vibrations and wave propagation problems are investigated using isogeometric analysis in [14]. Spectrum analysis of the method shows that the method significantly improves accuracy in the spectral calculation over the classical finite element method [13]. Further advantages of the method on spectral approximation properties are investigated in [22].

A duality principle, which induces a bijective map from spectral analysis to dispersion analysis, is established [23]. The spectral analysis for structural vibrations (eigenvalue problems) and the dispersion analysis for wave propagation are then unified. Although the cost per degree of freedom of isogeometric analysis is higher than for finite elements [10–12, 27], the dispersion error of is dramatically smaller than that of finite elements. However, we propose a blending scheme for isogeometric analysis which increases the convergence by two orders with respect to the mesh size. With this motivation, under the framework of unified analysis, we study the dispersion optimization of the isogeometric analysis.

Dispersion analysis for the Galerkin finite element methods has been studied actively in literature; see for example Thomson and Pinsky[33, 34], Ihlenburg and Babuska [24], Ainsworth [1], and others [18–20]. In [33], Thomson and Pinsky study the dispersive effects of the Galerkin methods with different local approximation basis (Legendre, spectral, and Fourier elements) for the Helmholtz equation and it is found that the choice of the basis has a negligible effect on the dispersion errors. In [1], a $2p$ convergence rate of the dispersion error is shown for arbitrary p-th order finite element

*Department of Applied Geology, Western Australian School of Mines, Curtin University, Kent Street, Bentley, Perth, WA 6102, Australia; Mineral Resources, Commonwealth Scientific and Industrial Research Organisation (CSIRO), Kensington, Perth, WA 6152, Australia. E-mail address: vmcalo@gmail.com. Tel: (+61)892664607

†Corresponding author. Department of Applied Geology, Western Australian School of Mines, Curtin University, Kent Street, Bentley, Perth, WA 6102, Australia. E-mail address: qdeng12@gmail.com. Tel: (+61)892662237

‡Department of Applied Geology, Western Australian School of Mines, Curtin University, Kent Street, Bentley, Perth, WA 6102, Australia. E-mail address: vladimir.puzyrev@gmail.com. Tel: (+61)892662237

methods. For the linear case, a fourth order superconvergence result is obtained by a modified integration rule for finite elements in [17].

As early as 1984, Marfurt in [25] conjectured that the most promising and cost-effective method for computational wave propagation is to employ a weighted average of the finite element and spectral element schemes. In 2010, Ainsworth and Wajid [3] introduced the optimal blending of these two schemes of arbitrary polynomial order. This optimal blending delivers two extra orders of convergence on the dispersion errors.

In 2016, a dispersion optimized edge-based mimetic finite difference method for Maxwell's equations in cold plasma is developed in [8]. They present a generalized form of mass lumping and an optimization procedure to reduce the numerical dispersion error from second to fourth order accuracy. In [35], they describe a similar result on dispersion by optimally blending finite-spectral element scheme for Maxwell's equations.

To evaluate the bilinear form, in the case of spectral and finite elements, Ainsworth and Wajid pointed out that spectral elements use the Gauss-Lobatto quadrature rule while finite elements use the Gauss-Legendre quadrature rule [3] on the same polynomial space. The optimal blending of spectral and finite elements is essentially a blending of the Gauss-Legendre and Gauss-Lobatto quadrature rules. Thus, this new blended quadrature rule minimizes the dispersion errors.

In this paper, we minimize the dispersion error for isogeometric analysis by blending quadrature rules appropriately while the eigenfunction errors do not degenerate. We study optimally blended quadratures for isogeometric analysis up to polynomial order seven. We minimize the dispersion error to obtain two additional orders of error convergence.

The rest of this paper is organized as follows. Section 2 presents the discretization of an eigenvalue problem and its generalized Pythagorean eigenvalue theorem. In Section 3, we present the discrete dispersion relation and derive the optimized dispersion error expansions for isogeometric analysis up to order seven. Dispersion and spectrum analysis are unified in the form of a Taylor expansion for the eigenvalue errors. Section 4 analyzes the error of the blending schemes and an a posteriori error estimator based on the superconvergence result of the eigenvalue error is derived. Section 5 presents numerical examples to demonstrate the performance of the proposed blending schemes. Section 6 describes our concluding remarks.

2. Problem setting. We consider stationary waves as described by the Helmholtz equation

$$\begin{aligned} \Delta u + \omega^2 u = 0 \quad &\text{in} \quad \Omega, \\ u = 0 \quad &\text{on} \quad \partial\Omega, \end{aligned} \tag{2.1}$$

where $\Omega \subset \mathbb{R}^d, d = 1, 2, 3$ is a bounded open domain with Lipschitz boundary, $\Delta = \nabla^2$ is the Laplacian and $\omega = \omega_f/c$ with ω_f being the frequency of a particular sinusoidal wave and c being the speed of sound of the medium. Denoting $\lambda = \omega^2$, in the view of duality and unified analysis of discrete approximations for wave propagation studied in [23], (2.1) is also posed as a second order elliptic eigenvalue problem: find λ and nonzero functions u such that

$$-\Delta u = \lambda u \quad \text{in} \quad \Omega. \tag{2.2}$$

The eigenvalue problem (2.2) has a countable set of eigenvalues $\lambda_j \in \mathbb{R}^+$ [31]

$$0 \le \lambda_1 \le \lambda_2 \le \lambda_3 \le \cdots \tag{2.3}$$

and an associated set of orthonormal eigenfunctions u_j

$$(u_j, u_k) = \delta_{jk}, \tag{2.4}$$

where $(\cdot,\cdot)$ denotes the L^2-inner product on Ω and $\delta_{lm} = 1$ when $l = m$ and zero otherwise and is known as the Kronecker delta.

2.1. Discretization. For an open set $S \subset \mathbb{R}^d$ with Lipschitz boundary, we denote by $W^{m,p}(S)$ a Sobolev space equipped with the norm $\|\cdot\|_{m,p,S}$ and the seminorm $|\cdot|_{m,p,S}$ where m is the order of the weak derivative and p corresponds to the p in L^p space. We use standard notation. If $p = 2$, we omit p and utilize $H^m(S)$ for Hilbert spaces and $H_0^m(S)$ for Hilbert spaces with functions vanishing at the boundary for $m > 0$. The variational formulation of (2.2) is to find $\lambda_j \in \mathbb{R}^+$ and $u_j \in H_0^1(\Omega)$ such that

$$a(u_j, v) = \lambda_j b(u_j, v) \quad \forall\ v \in H_0^1(\Omega), \tag{2.5}$$

where $a(w, v) = (\nabla w, \nabla v)$ and $b(w, v) = (w, v)$. Naturally, the normalized eigenfunctions are also orthogonal in the energy inner product

$$a(u_j, u_k) = \lambda_j b(u_j, u_k) = \lambda_j \delta_{jk}. \tag{2.6}$$

Assume that Ω is a cube and a uniform tensor product mesh of size $h_x > 0, h_y > 0, h_z > 0$ is placed on Ω with nodes located at $(h_x\mathbb{Z}, h_y\mathbb{Z}, h_z\mathbb{Z})$. We denote each element as K and its collection as $\mathcal{T}_h$ such that $\bar{\Omega} = \cup_{K\in\mathcal{T}_h} K$. Let $h = \max_{K\in\mathcal{T}_h} \text{diameter}(K)$. The Galerkin-type numerical methods seek $\lambda_j^h \in \mathbb{R}$ and $u_j^h \in V_h$ such that

$$a(u_j^h, v_h) = \lambda_j^h b(u_j^h, v_h) \quad \forall\ v_h \in V_h. \tag{2.7}$$

Different solution/trial spaces V_h lead to different numerical methods. Under this framework, we consider the following methods: finite element, spectral element, and isogeometric analysis. We utilize B-spline basis functions for isogeometric analysis. Abusing notation, let $\phi_a = \phi_a(x), a \in \mathbb{Z}$ be the basis functions for finite element, spectral element, and isogeometric analysis. Then $V_h = \text{span}\{\phi_a\}_{a\in\mathbb{Z}}$.

In the framework of finite elements, λ_j^h and u_j^h have the following properties [4, 5, 31]

$$|\lambda_j - \lambda_j^h| \le Ch^{2p} \qquad \text{and} \qquad \|u_j - u_j^h\|_{1,\Omega} \le Ch^p. \tag{2.8}$$

In practice, the integrals involved in $a(u_j^h, v_h)$ and $b(u_j^h, v_h)$ are evaluated numerically, that is, approximated by quadrature rules. On a reference element $\hat{K}$, a quadrature rule is of the form

$$\int_{\hat{K}} \hat{f}(\hat{\boldsymbol{x}})\ \mathrm{d}\hat{\boldsymbol{x}} \approx \sum_{l=1}^{N_q} \hat{\varpi}_l \hat{f}(\hat{n}_l), \tag{2.9}$$

where $\hat{\varpi}_l$ are the weights, $\hat{n}_l$ are the nodes, and N_q is the number of quadrature points. For each element K, we assume that there is an invertible affine map σ such that $K = \sigma(\hat{K})$, which leads to the correspondence between the functions on K and

$\hat{K}$. Assuming J_K is the corresponding Jacobian of the mapping, (2.9) induces a quadrature rule over the element K given by

$$\int_K f(\boldsymbol{x})\ \mathrm{d}\boldsymbol{x} \approx \sum_{l=1}^{N_q} \varpi_{l,K} f(n_{l,K}), \tag{2.10}$$

where $\varpi_{l,K} = \det(J_K)\hat{\varpi}_l$ and $n_{l,K} = \sigma(\hat{n}_l)$.

Applying quadrature rules to (2.7), we have the approximated form

$$\tilde{a}_h(\tilde{u}_j^h, v_h) = \tilde{\lambda}_j^h \tilde{b}_h(\tilde{u}_j^h, v_h) \quad \forall\ v_h \in V_h, \tag{2.11}$$

where

$$\tilde{a}_h(w, v) = \sum_{K\in\mathcal{T}_h} \sum_{l=1}^{N_q} \varpi_{l,K}^{(1)} \nabla w(n_{l,K}^{(1)}) \cdot \nabla v(n_{l,K}^{(1)}) \tag{2.12}$$

and

$$\tilde{b}_h(w, v) = \sum_{K\in\mathcal{T}_h} \sum_{l=1}^{N_q} \varpi_{l,K}^{(2)} w(n_{l,K}^{(2)}) v(n_{l,K}^{(2)}) \tag{2.13}$$

where $\{\varpi_{l,K}^{(1)}, n_{l,K}^{(1)}\}$ and $\{\varpi_{l,K}^{(2)}, n_{l,K}^{(2)}\}$ specify two (possibly different) quadrature rules.

With quadrature rules, if we substitute the basis functions for V_h into (2.11), this leads to the matrix eigenvalue problem

$$\mathbf{K}\tilde{\mathbf{U}}_j = \tilde{\lambda}_j^h \mathbf{M}\tilde{\mathbf{U}}_j \tag{2.14}$$

where $\mathbf{K}_{ab} = \tilde{a}_h(\phi_a, \phi_b), \mathbf{M}_{ab} = \tilde{b}_h(\phi_a, \phi_b)$, and $\tilde{\mathbf{U}}_j$ is the corresponding representation of the eigenvector as the coefficients of the basis functions.

2.2. Pythagorean eigenvalue theorem and its generalization. Denoting $\|\cdot\|_E$ the energy norm, the Pythagorean eigenvalue theorem [22] states

LEMMA 2.1. *For each discrete mode, with the normalization* $\|u_j\|_{0,\Omega} = 1$ *and* $\|u_j^h\|_{0,\Omega} = 1$, *we have*

$$\|u_j - u_j^h\|_E^2 = \lambda_j \|u_j - u_j^h\|_{0,\Omega}^2 + \lambda_j^h - \lambda_j. \tag{2.15}$$

Proof. This is proved in Strang and Fix [31]. ∎

Denoting $\|\cdot\|_{E,h}$ the energy norm evaluated by a quadrature rule (2.12), the generalized Pythagorean eigenvalue theorem is stated as follows

THEOREM 2.2. *For each discrete mode, with the normalization* $\|u_j\|_{0,\Omega} = 1$ *and* $\tilde{b}_h(\widetilde{u}_j^h, \widetilde{u}_j^h) = 1$, *we have*

$$\|u_j - \widetilde{u}_j^h\|_E^2 = \widetilde{\lambda}_j^h - \lambda_j + \lambda_j \|u_j - \widetilde{u}_j^h\|_{0,\Omega}^2 + \|\widetilde{u}_j^h\|_E^2 - \|\widetilde{u}_j^h\|_{E,h}^2 + \lambda_j \Big(1 - \|\widetilde{u}_j^h\|_{0,\Omega}^2\Big). \tag{2.16}$$

Proof. This is proved in [28]. ∎

REMARK 2.3. *The Pythagorean eigenvalue theorem reveals the properties of the numerical approximation of the eigenvalue problem when the inner products are fully represented in the discrete setting, while the generalized theorem accounts for the effect of the numerical integration.*

3. The discrete dispersion relation and dispersion optimization. In the linear element case, isogeometric analysis and finite elements coincide and result in the same discrete dispersion relation; see for example [1–3]. We start with quadratic elements and focus on the one-dimensional case with $\Omega = \mathbb{R}$ to illustrate the idea. Without loss of generality, we consider $\lambda_j = \lambda = \omega^2$ in this section.

Let $\phi_a = \phi_a(x)$ be a maximum continuity B-spline basis function for a given polynomial order. We seek an approximation of the form

$$U(x) = \sum_{a\in\mathbb{Z}} U^a \phi_a(x) \tag{3.1}$$

satisfying

$$\tilde{B}_h(U, v_h) = 0, \tag{3.2}$$

where $\tilde{B}_h(w, v) = \tilde{a}_h(w, v) - \omega^2 \tilde{b}_h(w, v)$.

Now, we denote by G_m the $m-$point Gauss-Legendre quadrature rule, by GL_m the $m-$point Gauss-Lobatto quadrature rule, and by O_p the optimal blending scheme for the p-th order isogeometric analysis with maximum continuity.

3.1. Quadratic elements. In particular, for the C^1 quadratic B-splines, applying G_3, one obtains the following equation for the value U^j of the approximation at node $x_j = jh, j \in \mathbb{Z}$

$$(20 + \Lambda^2)(U^{j-2} + U^{j+2}) + (40 + 26\Lambda^2)(U^{j-1} + U^{j+1}) - (120 - 66\Lambda^2)U^j = 0, \tag{3.3}$$

where $\Lambda = \omega h$. Assume the equation admits nontrivial Bloch wave [26] solutions in the form $U^j = e^{ij\mu_Q^{(2)}h}$, where $i^2 = -1$ and the subindex Q denotes the corresponding numerical quadrature, then (3.3) simplifies to

$$(20 + \Lambda^2)\cos^2(\mu_{G_3}^{(2)}h) + (20 + 13\Lambda^2)\cos(\mu_{G_3}^{(2)}h) + (-40 + 16\Lambda^2) = 0, \tag{3.4}$$

which is known as the *discrete dispersion relation* for the discrete method with a particular quadrature rule [1]. Solving (3.4) for $\mu_{G_3}^{(2)}h$ and writing the expression as a series in Λ, we obtain

$$\mu_{G_3}^{(2)}h = \Lambda - \frac{1}{1440}\Lambda^5 - \frac{1}{6720}\Lambda^7 + \mathcal{O}(\Lambda)^9. \tag{3.5}$$

Now applying GL_3, one obtains

$$(16 + \Lambda^2)(U^{j-2} + U^{j+2}) + (32 + 20\Lambda^2)(U^{j-1} + U^{j+1}) - (96 - 54\Lambda^2)U^j = 0, \tag{3.6}$$

which leads to the discrete dispersion relation

$$(16 + \Lambda^2)\cos^2(\mu_{GL_3}^{(2)}h) + (16 + 10\Lambda^2)\cos(\mu_{GL_3}^{(2)}h) + (-32 + 13\Lambda^2) = 0. \tag{3.7}$$

Solving (3.7) for $\mu_{GL_3}^{(2)}h$ and writing the expression as a series in Λ, we obtain

$$\mu_{GL_3}^{(2)}h = \Lambda + \frac{1}{2880}\Lambda^5 - \frac{1}{16128}\Lambda^7 + \mathcal{O}(\Lambda)^9. \tag{3.8}$$

Lastly, we apply G_2 to obtain

$$(24 + \Lambda^2)(U^{j-2} + U^{j+2}) + (48 + 32\Lambda^2)(U^{j-1} + U^{j+1}) - (72 - 39\Lambda^2)U^j = 0, \tag{3.9}$$

which leads to the discrete dispersion relation

$$(24+\Lambda^2)\cos^2(\mu_{G_2}^{(2)}h)+(24+16\Lambda^2)\cos(\mu_{G_2}^{(2)}h)+(-48+19\Lambda^2)=0. \tag{3.10}$$

Solving (3.10) for $\mu_{G_2}^{(2)}h$ and writing the expression as a series in Λ, we obtain

$$\mu_{G_2}^{(2)}h=\Lambda-\frac{1}{720}\Lambda^5-\frac{5}{24192}\Lambda^7+\mathcal{O}(\Lambda)^9. \tag{3.11}$$

REMARK 3.1. *G_3 integrates both the stiffness and mass terms exactly while GL_3 and G_2 integrate the stiffness terms exactly but under-integrate the mass ones. However, all of them yield the optimal order of convergence. Similar calculations also indicate that once the stiffness term is under-integrated, for example by GL_2 or G_1, the optimal convergence is lost. The impact of under-integration on convergence is discussed in [31] among others.*

The signs and coefficients of (3.5), (3.8), and (3.11) allow us to propose the following blendings

$$\frac{1}{3}G_3+\frac{2}{3}GL_3, \qquad 2G_3-G_2, \qquad \text{and} \qquad \frac{4}{5}GL_3+\frac{1}{5}G_2. \tag{3.12}$$

All of them lead to the discrete dispersion relation for the optimal scheme

$$(120+7\Lambda^2)\cos^2(\mu_{O_2}^{(2)}h)+(120+76\Lambda^2)\cos(\mu_{O_2}^{(2)}h)+(-240+97\Lambda^2)=0, \tag{3.13}$$

which gives the optimal dispersion error

$$\mu_{O_2}^{(2)}h=\Lambda-\frac{11}{120960}\Lambda^7-\frac{1}{345600}\Lambda^9+\mathcal{O}(\Lambda)^{11}. \tag{3.14}$$

REMARK 3.2. *The blending allows us to eliminate the fifth order error and gives a seventh order error. Moreover, the coefficient of the senventh order error is the sum of the corresponding ones in* (3.5)*,* (3.8)*, and* (3.11) *with weights specified in* (3.12)*. However, calculation shows that this is not the case for the coefficients of the ninth or higher orders.*

These blending schemes (3.12) integrate the stiffness terms exactly in one dimension and deliver two additional orders of convergence. They are optimal blending schemes since the dispersion error is minimized and provide superconvergence to the method. To see this, one can follow the work done for finite elements and spectral elements in [3]. The idea is to assign weights τ and $1-\tau$ to the two quadratures involved and determine τ to eliminate the coefficient of the leading term in the error expansion. Alternatively, one can optimize the dispersion error directly from the error expansion derived from the most general form

$$\begin{aligned}-\frac{1}{6}(U^{j-2}+U^{j+2})-\frac{1}{3}(U^{j-1}+U^{j+1})+U^j-\Lambda^2\big(\alpha(U^{j-2}+U^{j+2})\\ +\beta(U^{j-1}+U^{j+1})+(1-2\alpha-2\beta)U^j\big)=0.\end{aligned} \tag{3.15}$$

This leads to a dispersion error expansion

$$\begin{aligned}\mu_{O_2}^{(2)}h =&\Lambda + \left(-2\alpha - \frac{\beta}{2} + \frac{1}{8}\right)\Lambda^3 \\ &+ \frac{\left(34560\alpha^2 + 17280\alpha\beta - 3360\alpha + 2160\beta^2 - 1560\beta + 227\right)}{5760}\Lambda^5 \\ &+ \frac{\Lambda^7}{64512}\Big(- 1290240\alpha^3 - 967680\alpha^2\beta + 134400\alpha^2 - 241920\alpha\beta^2 + 147840\alpha\beta \\ &- 17808\alpha - 20160\beta^3 + 28560\beta^2 - 10164\beta + 1039\Big) + \mathcal{O}(\Lambda^9).\end{aligned} \tag{3.16}$$

To optimize the dispersion error, we set and solve

$$\begin{aligned}-2\alpha - \frac{\beta}{2} + \frac{1}{8} = 0 \\ 34560\alpha^2 + 17280\alpha\beta - 3360\alpha + 2160\beta^2 - 1560\beta + 227 = 0\end{aligned} \tag{3.17}$$

to obtain

$$\alpha = \frac{7}{720}, \qquad \beta = \frac{19}{90}, \tag{3.18}$$

which in return simplifies (3.16) to obtain the optimized dispersion error expression

$$\mu_{O_2}^{(2)}h = \Lambda - \frac{11}{120960}\Lambda^7 + \mathcal{O}(\Lambda)^9. \tag{3.19}$$

Thus, this alternative way leads to the same optimized dispersion error. In fact, values of α and β uniquely determine the coefficients in the blending schemes (3.12).

REMARK 3.3. *Partition of unity requires the coefficient of U^j in the mass term in* (3.15) *to be* $(1 - 2\alpha - 2\beta)$.

3.2. Cubic elements. Now we consider the cubic B-spline element case with maximum continuity, that is, C^2 basis functions. Similarly, applying G_4, GL_4, and G_3, we obtain the following discrete dispersion relations

$$\begin{aligned}0 =& (42 + \omega^2h^2)\cos^3(\mu_{G_4}^{(3)}h) + (504 + 60\omega^2h^2)\cos^2(\mu_{G_4}^{(3)}h) \\ &+ (126 + 297\omega^2h^2)\cos(\mu_{G_4}^{(3)}h) + (-672 + 272\omega^2h^2), \\ 0 =& (90 + 2\omega^2h^2)\cos^3(\mu_{GL_4}^{(3)}h) + (1080 + 129\omega^2h^2)\cos^2(\mu_{GL_4}^{(3)}h) \\ &+ (270 + 636\omega^2h^2)\cos(\mu_{GL_4}^{(3)}h) + (-1440 + 583\omega^2h^2), \\ 0 =& (120 + 3\omega^2h^2)\cos^3(\mu_{G_3}^{(3)}h) + (1440 + 171\omega^2h^2)\cos^2(\mu_{G_3}^{(3)}h) \\ &+ (360 + 849\omega^2h^2)\cos(\mu_{G_3}^{(3)}h) + (-1920 + 777\omega^2h^2),\end{aligned} \tag{3.20}$$

for the different cases. They lead to the dispersion error expansions given below

$$\begin{aligned}\mu_{G_4}^{(3)}h &= \Lambda - \frac{1}{60480}\Lambda^7 - \frac{1}{90720}\Lambda^9 + \mathcal{O}(\Lambda)^{11}, \\ \mu_{GL_4}^{(3)}h &= \Lambda - \frac{1}{100800}\Lambda^7 - \frac{11}{1814400}\Lambda^9 + \mathcal{O}(\Lambda)^{11}, \\ \mu_{G_3}^{(3)}h &= \Lambda - \frac{13}{604800}\Lambda^7 - \frac{37}{7257600}\Lambda^9 + \mathcal{O}(\Lambda)^{11}.\end{aligned} \tag{3.21}$$

The corresponding optimal blending schemes are

$$-\frac{3}{2}G_4+\frac{5}{2}GL_4,\qquad \frac{13}{3}G_4-\frac{10}{3}G_3,\qquad \text{and}\qquad \frac{13}{7}GL_4-\frac{6}{7}G_3, \tag{3.22}$$

which all result in the following optimized dispersion error expression

$$\mu_{O_3}^{(3)}h=\Lambda-\frac{1}{145152}\Lambda^9+\frac{19}{68428800}\Lambda^{11}+\mathcal{O}(\Lambda)^{13}. \tag{3.23}$$

REMARK 3.4. *There are other blending schemes which give the same optimized dispersion error expression. Here, we list a few*

$$\begin{aligned}&\frac{4}{35}GL_3+\frac{36}{35}G_2-\frac{1}{7}GL_2, && \frac{10}{49}G_3+\frac{234}{245}G_2-\frac{39}{245}GL_2,\\ &\frac{20}{7}G_3-\frac{52}{35}GL_3-\frac{13}{35}GL_2, && \frac{10}{7}GL_4-\frac{12}{35}GL_3-\frac{3}{35}GL_2.\end{aligned} \tag{3.24}$$

Also, as done for the quadratic case, one can assign α,β, and γ to the mass terms to derive the optimized dispersion error expression.

3.3. Higher-order elements. For higher order elements, the calculations and derivations become more complicated. In the following, we list our results up to order seven for isogeometric analysis with maximum continuity basis functions. As before, for orders $p=4,5,6,7$, we apply G_{p+1}, GL_{p+1}, and G_p to compute the integrals. Their corresponding dispersion error expressions are of the form

$$\mu_Q^{(p)}h=\Lambda-\epsilon_p^Q\Lambda^{2p+1}+\mathcal{O}(\Lambda^{2p+3}), \tag{3.25}$$

for $Q=G_{p+1}, GL_{p+1}, G_p$, while the optimized dispersion expressions are of the form

$$\mu_{O_p}^{(p)}h=\Lambda-\epsilon_p^o\Lambda^{2p+3}+\mathcal{O}(\Lambda^{2p+5}). \tag{3.26}$$

In Table 3.1, we list the coefficients ϵ_p^Q and ϵ_p^o for $p=4,5,6,7$. As before, the optimal blending schemes are not unique; we list a few of them below

$$\begin{aligned}&p=4 && -\frac{79}{5}G_5+\frac{84}{5}GL_5, && 22G_5-21G_4,\\ &p=5 && -174G_6+175GL_6, && 211G_6-210G_5,\\ &p=6 && -\frac{91177}{35}G_7+\frac{91212}{35}GL_7, && \frac{30414}{10}G_7-\frac{30404}{10}G_6,\\ &p=7 && -\frac{105103}{2}G_8+\frac{105105}{2}GL_8, && 60061G_8-60060G_7.\end{aligned} \tag{3.27}$$

These blending schemes can be rewritten as

$$G_{p+1}+C_{1,p}\cdot(GL_{p+1}-G_{p+1})\qquad\text{and}\qquad G_{p+1}+C_{2,p}\cdot(G_{p+1}-G_p) \tag{3.28}$$

where $C_{1,p}$ and $C_{2,p}$ depend on p and satisfy

$$pC_{2,p}-(p+1)C_{1,p}=0. \tag{3.29}$$

Thus, once the general form of one of them is obtained, the other one can be derived from (3.29).

REMARK 3.5. *The analysis of the possible generalization of the optimal blending schemes for isogeometric analysis with arbitrary order p of continuity order $k=1,\cdots,p-1$ is an open question and is still under investigation.*

p	G_{p+1}	GL_{p+1}	G_p	O_p
4	$\frac{3}{20 \cdot 9!}$	$\frac{79}{560 \cdot 9!}$	$\frac{11}{70 \cdot 9!}$	$\frac{317}{24 \cdot 11!}$
5	$\frac{5}{12 \cdot 11!}$	$\frac{29}{70 \cdot 11!}$	$\frac{211}{504 \cdot 11!}$	$\frac{35039}{420 \cdot 13!}$
6	$\frac{691}{420 \cdot 13!}$	$\frac{91177}{55440 \cdot 13!}$	$\frac{5069}{3080 \cdot 13!}$	$\frac{15479}{24 \cdot 15!}$
7	$\frac{35}{4 \cdot 15!}$	$\frac{105103}{12012 \cdot 15!}$	$\frac{60061}{6864 \cdot 15!}$	$\frac{91067}{15 \cdot 17!}$

TABLE 3.1

Leading order coefficients of the discrete dispersion relations for the different quadratures described and for different polynomial orders $p = 4, 5, 6, 7$.

3.4. Extension to multidimension. The extension is similar to the extension done for finite elements in [3]. The conclusion is that the optimal blending for arbitrary dimension coincides with the one we derive above for the one-dimensional case and is independent of the number of spatial dimensions.

Let $d \geq 1$ be the dimension that can be greater than three. Assume that a uniform tensor product grid of size h_{x_l} on each dimension is placed on $\Omega \subset \mathbb{R}^d$. Define the basis function as the tensor product of the basis functions in one dimension

$$\phi_{a_1}(x_1)\phi_{a_2}(x_2)\cdots\phi_{a_d}(x_d).$$

We seek a solution of the form

$$U = \prod_{1\leq m\leq d} U(x_m), \tag{3.30}$$

where each $U(x_m)$ has a one dimensional representation (3.1). Thus, we have

$$\tilde{b}_h\big(U, \phi_{a_1}(x_1)\cdots\phi_{a_d}(x_d)\big) = \prod_{1\leq m\leq d} \tilde{b}_h\big(U(x_m), \phi_{a_m}(x_m)\big). \tag{3.31}$$

Suppose that on each dimension k, it satisfies (3.2), then

$$\tilde{a}_h\big(U(x_k), \phi_{a_k}(x_k)\big) - \omega_k^2 \tilde{b}_h\big(U(x_k), \phi_{a_k}(x_k)\big) = 0. \tag{3.32}$$

Then by applying the one dimensional equation (3.32), we get

$$\begin{aligned}
\tilde{a}_h\big(U, \phi_{a_1}(x_1)\cdots\phi_{a_d}(x_d)\big) &= \sum_{k=1}^{d} \Big(\tilde{a}_h\big(U(x_k), \phi_{a_k}(x_k)\big) \prod_{m\neq k, 1\leq m\leq d} \tilde{b}_h\big(U(x_m), \phi_{a_m}(x_m)\big)\Big) \\
&= \sum_{k=1}^{d} \Big(\omega_k^2 \prod_{1\leq m\leq d} \tilde{b}_h\big(U(x_m), \phi_{a_m}(x_m)\big)\Big) \\
&= \Big(\sum_{k=1}^{d} \omega_k^2\Big)\Big(\prod_{1\leq m\leq d} \tilde{b}_h\big(U(x_m), \phi_{a_m}(x_m)\big)\Big).
\end{aligned} \tag{3.33}$$

The multi-dimension problem is to find U satisfying for all the basis functions

$$\tilde{a}_h\big(U, \phi_{a_1}(x_1)\cdots\phi_{a_d}(x_d)\big) - \omega^2 \tilde{b}_h\big(U, \phi_{a_1}(x_1)\cdots\phi_{a_d}(x_d)\big) = 0. \tag{3.34}$$

Plugging (3.31) and (3.33) into (3.34), the multidimensional problem admits a nontrivial solution provided that

$$\omega^2 = \sum_{k=1}^{d} \omega_k^2. \tag{3.35}$$

Thus, the schemes we propose can be extended to multidimensional problems. The corresponding optimized dispersion error expression for multidimensional problems can be deduced from (3.26) and (3.35), which is

$$(\mu_{O_p}^{(p)})^2 = \omega^2 + \mathcal{O}(\omega^{2p+4}h^{2p+2}). \tag{3.36}$$

3.5. Duality with spectrum analysis. There is a symmetry between (2.1) and (2.2). The duality between spectrum analysis and dispersion analysis has been established in [23]. Now, we denote the approximate frequencies by $\kappa_Q^{(p)}$, where Q specifies the quadrature rule. For spectrum analysis of the quadratic case, replacing Λ with $\kappa_Q^{(p)}h$ and $\mu_Q^{(p)}$ with ω, we obtain

$$\begin{aligned}
&\kappa_{G_3}^{(2)}h = \sqrt{\frac{40-20\cos(\omega h)-20\cos^2(\omega h)}{16+13\cos(\omega h)+\cos^2(\omega h)}}, \kappa_{GL_3}^{(2)}h = \sqrt{\frac{32-16\cos(\omega h)-16\cos^2(\omega h)}{13+10\cos(\omega h)+\cos^2(\omega h)}},\\
&\kappa_{G_2}^{(2)}h = \sqrt{\frac{48-24\cos(\omega h)-24\cos^2(\omega h)}{19+16\cos(\omega h)+\cos^2(\omega h)}}, \kappa_{O_2}^{(2)}h = \sqrt{\frac{120\big(2-\cos(\omega h)-\cos^2(\omega h)\big)}{97+76\cos(\omega h)+7\cos^2(\omega h)}}.
\end{aligned} \tag{3.37}$$

Applying the Taylor expansion on these expressions gives

$$\begin{aligned}
&\kappa_{G_3}^{(2)}h = \omega h + \frac{1}{1440}(\omega h)^5 + \mathcal{O}(\omega h)^7, \kappa_{GL_3}^{(2)}h = \omega h - \frac{1}{2880}(\omega h)^5 + \mathcal{O}(\omega h)^7,\\
&\kappa_{G_2}^{(2)}h = \omega h + \frac{1}{720}(\omega h)^5 + \mathcal{O}(\omega h)^7, \kappa_{O_2}^{(2)}h = \omega h + \frac{11}{120960}(\omega h)^7 + \mathcal{O}(\omega h)^9.
\end{aligned} \tag{3.38}$$

Similarly, this spectrum analysis can be done for cubic and higher order methods. In general, we obtain error expressions for $p = 2, \cdots, 7$ in the forms

$$\kappa_Q^{(p)}h = \omega h + \epsilon_p^Q(\omega h)^{2p+1} + \mathcal{O}(\omega h)^{2p+3}, \tag{3.39}$$

for $Q = G_{p+1}, GL_{p+1}, G_p$ and

$$\kappa_{O_p}^{(p)}h = \omega h + \epsilon_p^o(\omega h)^{2p+3} + \mathcal{O}(\omega h)^{2p+5}. \tag{3.40}$$

for the optimal schemes. For the cubic case, coefficients $\epsilon_3^o = 1/145152$ and $\epsilon_3^Q = 1/60480, 1/100800, 13/604800$ for $Q = G_3, GL_3$, and G_2, respectively, while for $p = 4, 5, 6, 7$, coefficients ϵ_p^Q and ϵ_p^o are given in Table 3.1. According to subsection 3.4, extension to multidimensions gives

$$(\kappa_{O_p}^{(p)})^2 = \omega^2 + \mathcal{O}(\omega^{2p+4}h^{2p+2}). \tag{3.41}$$

REMARK 3.6. *Equations* (3.39) *with* (3.25) *and* (3.40) *with* (3.26) *reveal the duality principle of dispersion and spectrum analysis in the error expansion form. The duality principle remains valid for the optimal blending schemes. The different signs of the coefficients* ϵ_p^Q *and* ϵ_p^o *in the error expressions are consequences of duality. Also, the first equation in* (3.37) *is given in [23].*

4. Error analysis. In the previous section, we study the dispersion error for a single eigenvalue case. The results hold true for all the eigenvalues for which ωh is sufficiently small. Now, for the purpose of error analysis, we consider again eigenpairs (λ_j, u_j). Throughout this paper, we refer to (λ_j, u_j) as the exact eigenpair, (λ_j^h, u_j^h) as the approximate eigenpair when the inner product is not modified by the numerical quadrature, and $(\tilde{\lambda}_j^h, \tilde{u}_j^h)$ the approximate eigenpair modified by the numerical quadrature. From [5, 31], the errors for both (λ_j^h, u_j^h) and $(\tilde{\lambda}_j^h, \tilde{u}_j^h)$ are of the forms (2.8) and (**??**) under the framework of finite element analysis. We now estimate the error of $(\tilde{\lambda}_j^h, \tilde{u}_j^h)$ under the framework of isogeometric analysis such that they are of the forms

$$|\lambda_j - \tilde{\lambda}_j^h| \leq Ch^{2p+2} \quad \text{and} \quad \|u_j - \tilde{u}_j^h\|_{1,\Omega} \leq Ch^p. \tag{4.1}$$

4.1. Eigenvalue estimates. As noted by Banerjee in 1992 [4], one only obtains an order of $2p$ for the eigenvalue errors by using the standard quadrature rules, such as Gauss or Lobatto rules. This confirms our theoretical finding of (3.39) for orders $p = 2, \cdots, 7$ and we conjecture that this is true for arbitrary order. To see this, (3.39) gives the following estimate

$$|\kappa_Q^{(p)} - \omega| \leq Ch^{2p}\lambda_j^p,$$

which yields the $2p$ order convergence for the eigenvalues. Details are similar to the proof of the following theorem.

Up to order $p = 7$, eigenvalues errors are represented by the dispersion error expansions in Section 3. We have the following theorem.

THEOREM 4.1. *For a fixed $j \geq 1$ and $p = 1, \cdots, 7$, assume $\tilde{\lambda}_j^h = (\kappa_{O_p}^{(p)})^2$. For sufficiently small h, we have*

$$|\lambda_j - \tilde{\lambda}_j^h| \leq Ch^{2p+2}\lambda_j^{p+2}. \tag{4.2}$$

Proof. For order $p = 1$, this is shown in [3]. For order higher than 7, we conjecture that this is also true. Now, for orders $p = 2, \cdots, 7$, we have the error representation (3.40). Since $\lambda_j = \omega^2$, for sufficiently small h, equation (3.41) immediately gives us the desired result. This shows that we obtain two extra orders of convergence for the eigenvalue errors for the optimally blended schemes. ∎

4.2. Eigenfunction estimates. In this section, we establish the non-degeneracy of the eigenfunction errors. First, we establish the coercivity of the bilinear forms (2.12) and (2.13).

LEMMA 4.2. *Given the blending scheme of the form* (3.28)*, the bilinear forms* (2.12) *and* (2.13) *are coercive, that is, there exists a constant $\tilde{\alpha} > 0$ independent of h such that*

$$\forall v_h \ \in V_h, \qquad \tilde{\alpha}|v_h|_{1,\Omega}^2 \leq \tilde{a}_h(v_h, v_h) \quad \textit{and} \quad \tilde{\alpha}\|v_h\|_{0,\Omega}^2 \leq \tilde{b}_h(v_h, v_h). \tag{4.3}$$

Proof. We consider the blending scheme $G_{p+1} + C_{2,p} \cdot (G_{p+1} - G_p)$ for p-th order isogeometric analysis of maximum continuity and the proof for the other one in (3.28) is similar. Since G_{p+1} and G_p are exact for polynomial spaces of order $2p+1$ and $2p-1$, respectively, the blending scheme is exact for polynomial space of order $2p-1$. Hence, by Theorem 4.1.2 in [9], the bilinear form $\tilde{a}_h(\cdot, \cdot)$ is coercive.

Now, for $\tilde{b}_h(v_h, v_h)$, if the quadrature rule applied to the integral is G_{p+1}, then $\tilde{b}_h(v_h, v_h) = \|v_h\|_{0,\Omega}^2$. In the following, we treat the quadrature rules as operators on integrals and let $\mathcal{I}$ be the identity operator. We calculate

$$\begin{aligned}\tilde{b}_h(v_h, v_h) &= \big(G_{p+1} + C_{2,p} \cdot (G_{p+1} - G_p)\big) \circ \int_\Omega v_h^2 \, \mathrm{d}\boldsymbol{x} \\ &= \big(G_{p+1}\big) \circ \int_\Omega v_h^2 \, \mathrm{d}\boldsymbol{x} + C_{2,p} \cdot \big(G_{p+1} - G_p\big) \circ \int_\Omega v_h^2 \, \mathrm{d}\boldsymbol{x} \\ &= \|v_h\|_{0,\Omega}^2 + C_{2,p} \cdot \big(G_{p+1} - \mathcal{I}\big) \circ \int_\Omega v_h^2 \, \mathrm{d}\boldsymbol{x} + C_{2,p} \cdot \big(\mathcal{I} - G_p\big) \circ \int_\Omega v_h^2 \, \mathrm{d}\boldsymbol{x}\end{aligned}$$

By Lemma 3.1 in [5], we have

$$\begin{aligned}\big|\big(G_{p+1} - \mathcal{I}\big) \circ \int_\Omega v_h^2 \, \mathrm{d}\boldsymbol{x}\big| &\leq C \cdot h^{2p+2} \|v_h\|_{0,\Omega}^2 \\ \big(\mathcal{I} - G_p\big) \circ \int_\Omega v_h^2 \, \mathrm{d}\boldsymbol{x} &\leq C \cdot h^{2p} \|v_h\|_{0,\Omega}^2.\end{aligned}$$

Thus, for sufficiently small h, we have a constant $0 < \tilde{\alpha} < 1$ such that

$$\tilde{b}_h(v_h, v_h) \geq \tilde{\alpha} \|v_h\|_{0,\Omega}^2,$$

which completes the proof. ∎

The boundedness of $\tilde{b}_h(\cdot, \cdot)$ is a consequence of the proof. With coercivity, we immediately conclude that the eigenvalues of (2.11) are positive. Now, before we establish the eigenfunction error estimate, we present the following lemma.

LEMMA 4.3. *Suppose* $\Omega = [0, 1] \times [0, 1] \subset \mathbb{R}^2$. *We have*

$$\|u_j - \tilde{u}_j^h\|_{0,\Omega} \leq \frac{h}{\sqrt{2}} |u_j - \tilde{u}_j^h|_{1,\Omega}. \tag{4.4}$$

Proof. For simplicity, we denote $e(x, y) = u_j - \tilde{u}_j^h$. Then $e \in H_0^1(\Omega)$ since $u \in H_0^1(\Omega)$ and $\tilde{u}_j^h \in H_0^1(\Omega)$. We prove the inequality for $e \in C_0^\infty(\Omega)$ since any function in $H_0^1(\Omega)$ is the limit in $H^1(\Omega)$ of a sequence in $C_0^\infty(\Omega)$ [32]. For $0 < y < 1$, we have

$$e(x, y) = e(0, y) + \int_0^x \frac{\partial e(\xi, y)}{\partial x} \, \mathrm{d}\xi = \int_0^x \frac{\partial e(\xi, y)}{\partial x} \, \mathrm{d}\xi. \tag{4.5}$$

Denote the discretization in the $x-$dimension as $0 = x_0 < x_1 < \cdots < x_{N+1} = x$ and we denote N_0 the maximum index, such that, when $x_0 = x = 1$. We let $h_{x,l} = x_{l+1} - x_l$ and define the characteristic function χ_l for this segment as

$$\chi_l(x) = \begin{cases} 1 & \text{if} \quad x_l < x < x_{l+1} \\ 0 & \text{otherwise} \end{cases}. \tag{4.6}$$

Thus, by Cauchy-Schwarz inequality, we obtain

$$\begin{aligned}
\|u_j-\tilde{u}_j^h\|_{0,\Omega}^2 &= \int_\Omega |e|^2 \,\mathrm{d}x\mathrm{d}y = \int_0^1\int_0^1 \Big|\int_0^x \frac{\partial e(\xi,y)}{\partial x}\,\mathrm{d}\xi\Big|^2\,\mathrm{d}x\mathrm{d}y \\
&\le \int_0^1\int_0^1 \sum_{l=0}^{N}\Big|\int_{x_l}^{x_{l+1}} \frac{\partial e(\xi,y)}{\partial x}\,\mathrm{d}\xi\Big|^2\,\mathrm{d}x\mathrm{d}y \\
&\le \int_0^1\int_0^1 \sum_{l=0}^{N}\Big(h_{x,l}\int_{x_l}^{x_{l+1}} \Big|\frac{\partial e(\xi,y)}{\partial x}\Big|^2\,\mathrm{d}\xi\Big)\,\mathrm{d}x\mathrm{d}y \\
&\le \int_0^1 \sum_{l=0}^{N_0}\Big(\int_0^1 \chi_l(x)h_{x,l}\mathrm{d}x\int_{x_l}^{x_{l+1}} \Big|\frac{\partial e(\xi,y)}{\partial x}\Big|^2\,\mathrm{d}\xi\Big)\,\mathrm{d}y \\
&= \int_0^1 \sum_{l=0}^{N_0}\Big(\int_0^1 \chi_l(x)h_{x,l}\mathrm{d}x\int_{x_l}^{x_{l+1}} \Big|\frac{\partial e(\xi,y)}{\partial x}\Big|^2\,\mathrm{d}\xi\Big)\,\mathrm{d}y \\
&= \int_0^1 \sum_{l=0}^{N_0}\Big(h_{x,l}^2\int_{x_l}^{x_{l+1}} \Big|\frac{\partial e(\xi,y)}{\partial x}\Big|^2\,\mathrm{d}\xi\Big)\,\mathrm{d}y \\
&\le h^2\int_0^1 \sum_{l=0}^{N_0}\Big(\int_{x_l}^{x_{l+1}} \Big|\frac{\partial e(\xi,y)}{\partial x}\Big|^2\,\mathrm{d}\xi\Big)\,\mathrm{d}y \\
&= h^2\int_0^1\int_0^1 \Big|\frac{\partial e(\xi,y)}{\partial x}\Big|^2\,\mathrm{d}\xi\mathrm{d}y.
\end{aligned} \tag{4.7}$$

Similarly, we obtain

$$\|u_j-\tilde{u}_j^h\|_{0,\Omega}^2 \le h^2\int_0^1\int_0^1 \Big|\frac{\partial e(x,\xi)}{\partial y}\Big|^2\,\mathrm{d}\xi\mathrm{d}x. \tag{4.8}$$

Adding these two inequalities and taking the square root of both sides give us the desired result. □

REMARK 4.4. *The proof for general Ω, including three-dimension domain, is analogous and a constant depending on Ω may appear [32]. Also, for non-homogeneous Dirichlet boundary conditions, we also have $e \in H_0^1(\Omega)$. Hence, Lemma 4.3 is also valid for non-homogeneous Dirichlet boundary conditions.*

THEOREM 4.5. *For a fixed $j \ge 1$, assume that u_j and $\tilde{u}_j^h$ are normalized, that is, $b(u_j,u_j)=1$ and $\tilde{b}_h(\tilde{u}_j^h,\tilde{u}_j^h)=1$, and the signs of eigenfunctions of u_j and $\tilde{u}_j^h$ are chosen such that $b(u_j,\tilde{u}_j^h)>0$. Then for sufficiently small h, we have the estimate*

$$|u_j-\tilde{u}_j^h|_{1,\Omega} \le Ch^p. \tag{4.9}$$

Proof. With the normalization $b(u_j,u_j)=1$ and $\tilde{b}_h(\tilde{u}_j^h,\tilde{u}_j^h)=1$, by (2.5) and (2.11) we have

$$a(u_j,u_j)=\lambda_j b(u_j,u_j)=\lambda_j, \qquad \tilde{a}_h(\tilde{u}_j^h,\tilde{u}_j^h)=\tilde{\lambda}_j^h\tilde{b}_h(\tilde{u}_j^h,\tilde{u}_j^h)=\tilde{\lambda}_j^h. \tag{4.10}$$

Analogously to the derivations described in [29, 30], we estimate the modified bilinear forms, that is, for $v,w\in V_h$ there holds

$$\begin{aligned}
|a(v,w)-\tilde{a}_h(v,w)| &\le Ch^{2p}\|v\|_{p,\Omega}\|w\|_{p,\Omega}, \\
|b(v,w)-\tilde{b}_h(v,w)| &\le Ch^{2p}\|v\|_{p,\Omega}\|w\|_{p,\Omega}.
\end{aligned} \tag{4.11}$$

Thus, for a fixed j, by definition and using (2.5) and (2.11), we obtain

$$\begin{aligned}
|u_j - \tilde{u}_j^h|_{1,\Omega}^2 &= a(u_j - \tilde{u}_j^h, u_j - \tilde{u}_j^h) \\
&= a(u_j, u_j) - 2a(u_j, \tilde{u}_j^h) + a(\tilde{u}_j^h, \tilde{u}_j^h) \\
&= \lambda_j - 2\lambda_j b(u_j, \tilde{u}_j^h) + \tilde{\lambda}_j^h + \big(a(\tilde{u}_j^h, \tilde{u}_j^h) - \tilde{a}_h(\tilde{u}_j^h, \tilde{u}_j^h)\big) \\
&= \lambda_j\big(2 - 2b(u_j, \tilde{u}_j^h)\big) + \tilde{\lambda}_j^h - \lambda_j + \big(a(\tilde{u}_j^h, \tilde{u}_j^h) - \tilde{a}_h(\tilde{u}_j^h, \tilde{u}_j^h)\big) \\
&= \lambda_j \|u_j - \tilde{u}_j^h\|_{0,\Omega}^2 + \tilde{\lambda}_j^h - \lambda_j \\
&\quad + \big(a(\tilde{u}_j^h, \tilde{u}_j^h) - \tilde{a}_h(\tilde{u}_j^h, \tilde{u}_j^h)\big) + \lambda_j\big(\tilde{b}_h(\tilde{u}_j^h, \tilde{u}_j^h) - b(\tilde{u}_j^h, \tilde{u}_j^h)\big).
\end{aligned} \tag{4.12}$$

Rearranging terms and taking absolute value yields

$$\begin{aligned}
\Big||u_j - \tilde{u}_j^h|_{1,\Omega}^2 - \lambda_j \|u_j - \tilde{u}_j^h\|_{0,\Omega}^2\Big| &= \Big|\tilde{\lambda}_j^h - \lambda_j + \big(a(\tilde{u}_j^h, \tilde{u}_j^h) - \tilde{a}_h(\tilde{u}_j^h, \tilde{u}_j^h)\big) \\
&\qquad + \lambda_j\big(\tilde{b}_h(\tilde{u}_j^h, \tilde{u}_j^h) - b(\tilde{u}_j^h, \tilde{u}_j^h)\big)\Big| \\
&\le |\tilde{\lambda}_j^h - \lambda_j| + |a(\tilde{u}_j^h, \tilde{u}_j^h) - \tilde{a}_h(\tilde{u}_j^h, \tilde{u}_j^h)| \\
&\qquad + \lambda_j |\tilde{b}_h(\tilde{u}_j^h, \tilde{u}_j^h) - b(\tilde{u}_j^h, \tilde{u}_j^h)|.
\end{aligned} \tag{4.13}$$

Lemma 4.3 gives the following inequality

$$\|u_j - \tilde{u}_j^h\|_{0,\Omega} \le Ch|u_j - \tilde{u}_j^h|_{1,\Omega}. \tag{4.14}$$

By applying Theorem 4.1, (4.4), and (4.11), for sufficiently small h, we have

$$\tilde{C}|u_j - \tilde{u}_j^h|_{1,\Omega}^2 \le \Big||u_j - \tilde{u}_j^h|_{1,\Omega}^2 - \lambda_j \|u_j - \tilde{u}_j^h\|_{0,\Omega}^2\Big| \le Ch^{2p}. \tag{4.15}$$

Taking the square root on both sides completes the proof. ∎

Also, in these derivations the energy norm is the H^1-seminorm, thus we also have

$$\|u_j - \tilde{u}_j^h\|_E \le Ch^p. \tag{4.16}$$

By using Lemma 4.3, we obtain an estimation for eigenfunction errors in L^2-norm

$$\|u_j - \tilde{u}_j^h\|_{0,\Omega} \le Ch^{p+1}. \tag{4.17}$$

Now, we revisit the generalized Pythagorean eigenvalue theorem to derive an a posteriori error estimator for the eigenfunctions. We present the result in the form of the following corollary.

COROLLARY 4.6. *Assume for each discrete mode, the normalization* $\|u_j\|_{0,\Omega} = 1$ *and* $\tilde{b}_h(\widetilde{u}_j^h, \widetilde{u}_j^h) = 1$. *For sufficiently small* h, *we have the following error estimator with lower and upper bounds for the eigenfunction errors in the energy norm*

$$(1-\rho)R(\widetilde{\lambda}_j^h, \widetilde{u}_j^h) \le \|u_j - \widetilde{u}_j^h\|_E \le (1+\rho)R(\widetilde{\lambda}_j^h, \widetilde{u}_j^h), \tag{4.18}$$

where $0 < \rho < 1$ *and the residual is defined as*

$$R(\widetilde{\lambda}_j^h, \widetilde{u}_j^h) = \sqrt{a(\tilde{u}_j^h, \tilde{u}_j^h) - \tilde{\lambda}_j^h b(\tilde{u}_j^h, \tilde{u}_j^h)}. \tag{4.19}$$

Proof. This result can be achieved by applying the superconvergence property of the eigenvalue errors derived in subsection 4.1 to the generalized Pythagorean eigenvalue theorem. Alternatively, we derive this as follows.

$$\begin{aligned}
\|u_j - \widetilde{u}_j^h\|_E^2 &= a(u_j - \widetilde{u}_j^h, u_j - \widetilde{u}_j^h) \\
&= a(u_j, u_j) - 2\lambda_j b(u_j, \widetilde{u}_j^h) + a(\widetilde{u}_j^h, \widetilde{u}_j^h) \\
&= \lambda_j b(u_j, u_j) - 2\lambda_j b(u_j, \widetilde{u}_j^h) + \lambda_j b(\tilde{u}_j^h, \tilde{u}_j^h) - \lambda_j b(\tilde{u}_j^h, \tilde{u}_j^h) + a(\widetilde{u}_j^h, \widetilde{u}_j^h) \\
&= \lambda_j \|u_j - \tilde{u}_j^h\|_{0,\Omega}^2 - \lambda_j b(\tilde{u}_j^h, \tilde{u}_j^h) + a(\widetilde{u}_j^h, \widetilde{u}_j^h) - \tilde{\lambda}_j^h b(\tilde{u}_j^h, \tilde{u}_j^h) + \tilde{\lambda}_j^h b(\tilde{u}_j^h, \tilde{u}_j^h) \\
&= \lambda_j \|u_j - \tilde{u}_j^h\|_{0,\Omega}^2 + (\tilde{\lambda}_j^h - \lambda_j)\|\tilde{u}_j^h\|_{0,\Omega}^2 + R^2(\widetilde{\lambda}_j^h, \widetilde{u}_j^h).
\end{aligned}$$

Now, using Theorem 4.1 and (4.17), we have

$$\lambda_j \|u_j - \tilde{u}_j^h\|_{0,\Omega}^2 + (\tilde{\lambda}_j^h - \lambda_j)\|\tilde{u}_j^h\|_{0,\Omega}^2 \leq Ch^{2p+2}, \tag{4.20}$$

which is of higher order than $\|u_j - \widetilde{u}_j^h\|_E^2$. Thus, the error is dominated by the residual $R(\widetilde{\lambda}_j^h, \widetilde{u}_j^h)$. Hence, for sufficiently small h, we have the desired result. ∎

REMARK 4.7. *This a posteriori error estimator strongly relies on the superconvergence result on uniform meshes.*

5. Numerical experiments. For more detailed numerical results, we refer the reader to the paper [28], in which comparisons with finite elements and spectral elements are made. We focus on isogeometric analysis and study the convergence of the eigenvalue (EV) and eigenfunction (EF) errors in one and two dimensions. Three or higher dimensions are simple extensions as discussed in Section 3.4.

5.1. Convergence study in one dimension. We consider the classic one dimensional second order elliptic eigenvalue problem (2.2) with eigenvalues and eigenfunctions $\lambda_j = \pi^2 j^2, u_j = \sqrt{2}\sin(j\pi x), j = 1, 2, \cdots$. This is the same example studied in [22, 28] among many others. We assume that once the eigenvalue problem is solved, the numerical eigenvalues λ_j^h and $\tilde{\lambda}_j^h$ are sorted in ascending order and paired with the true eigenvalues λ_j.

First of all, for p-th order isogeometric analysis with maximum continuity, that is C^{p-1}, the quadrature rule G_{p+1} approximates both stiffness and mass matrices exactly while GL_{p+1}, G_p, and O_p integrate the stiffness matrices exactly but underintegrate the mass matrix. Despite these differences, all of them lead to accurate approximations to the eigenfunctions. Figure 5.1 shows the plots of the numerical approximations of eigenfunctions u_1 and u_{10} using C^1 quadratic isogeometric analysis with two elements for u_1 and twenty elements for u_{10}. As a comparison, Figure 5.2 shows the numerical approximation of u_{10} using C^2 cubic isogeometric analysis with twenty elements.

5.1.1. Eigenvalue errors. The analysis of eigenvalue errors done in Section 4.1 is verified numerically in this subsection. While in [28] we show better approximation properties when using isogeometric analysis over finite elements and spectral elements for the same problem, the optimally blended quadrature rules proposed in this paper yield two additional error convergence orders within the framework of isogeometric analysis.

Figure 5.3 shows the dispersion errors for the eigenvalues with isogeometric analysis for C^1 quadratic elements. The mesh sizes used are 20, 40, 80, 160, and 320. The figure shows two extra orders of convergence in the error for the eigenvalues λ_3 and

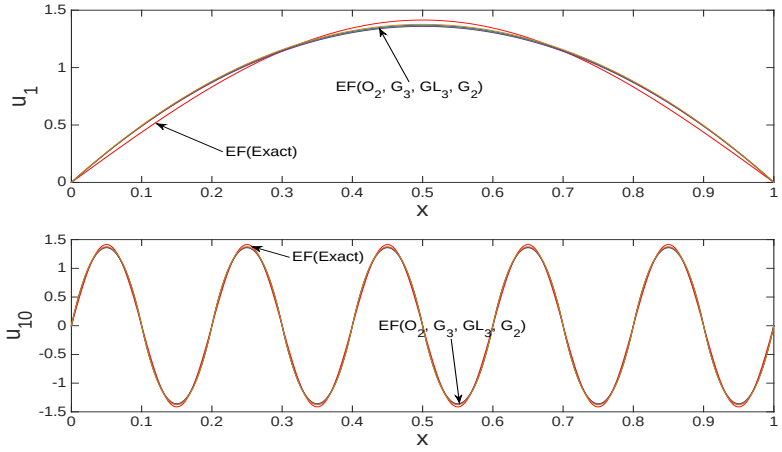

FIG. 5.1. *Eigenfunctions u_1 and u_{10} using C^1 quadratic isogeometric analysis with quadrature rules G_3, GL_3, G_2, and O_2.*

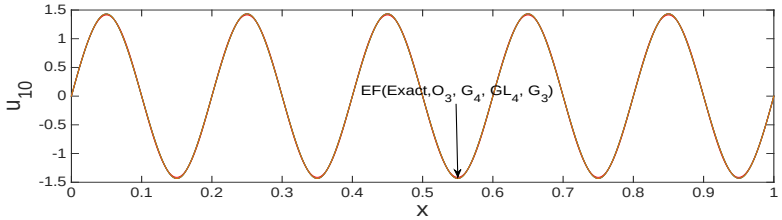

FIG. 5.2. *Eigenfunction u_{10} using C^2 cubic isogeometric analysis with quadrature rules G_4, GL_4, G_3, and O_3.*

λ_{11}. With both stiffness and mass matrices integrated exactly by G_3, the eigenvalue errors converge at the rate of h^4, while a slight modification of the quadrature rule, which is easily realized by optimally blended quadrature rule O_2 leads to a convergence rate of order six.

Further inspection of Figure 5.3 reveals that the eigenvalue errors are generally smaller for the case of GL_3 than those of G_3 and smaller for G_3 than for G_2. This observation confirms the theoretical analysis we present in Section 3 . The leading order terms in the Taylor expansions of the dispersion error (3.8) for GL_3, (3.5) for G_3, and (3.11) for G_2 have absolute values of $1/2880$, $1/1440$, and $1/720$, respectively. That is, $1/2880 < 1/1440 < 1/720$. Figure 5.4 shows similar results for C^2 cubic isogeometric analysis while Figure 5.5 shows these for C^3 quartic and C^4 quintic isogeometric analysis. These numerical results confirm the eigenvalue error analysis we discuss in Section 4.1.

5.1.2. Eigenfunction errors. In this subsection, we verify numerically the analysis of Section 4.2. While Figures 5.1 and 5.2 show several sample plots of approximate and exact eigenfunctions, we show in this subsection convergence rates of the eigenfunction errors.

As the analysis predicts, the error in the eigenfunctions for the optimally blended schemes does not exhibit two extra orders of superconvergence. For the H^1-seminorm, all schemes yield a convergence of order p for p-th order isogeometric elements with maximum continuity C^{p-1} at element interfaces.

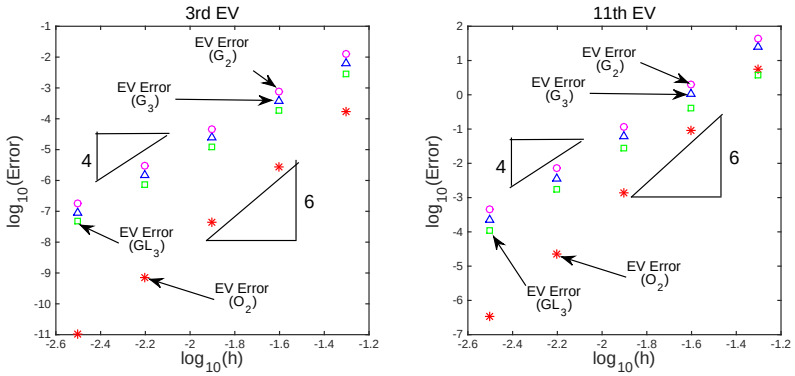

FIG. 5.3. *Dispersion errors for eigenvalues λ_3 and λ_{11} using C^1 quadratic isogeometric analysis with quadrature rules G_3, GL_3, G_2, and O_2.*

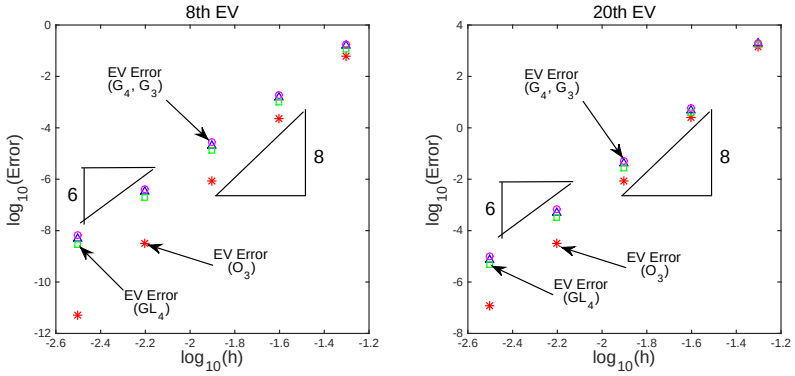

FIG. 5.4. *Dispersion errors for eigenvalues λ_8 and λ_{20} using C^2 cubic isogeometric analysis with quadrature rules G_4, GL_4, G_3, and O_3.*

mesh	O_2	G_3	GL_3	G_2
20	8.007409E-02	8.007620E-02	8.007355E-02	8.007966E-02
40	1.962886E-02	1.962889E-02	1.962885E-02	1.962894E-02
80	4.882983E-03	4.882983E-03	4.882983E-03	4.882984E-03
160	1.219233E-03	1.219233E-03	1.219233E-03	1.219233E-03
320	3.047138E-04	3.047138E-04	3.047138E-04	3.047138E-04
Order	2.01	2.01	2.01	2.01

TABLE 5.1

Eigenfunction H^1-seminorm errors for u_3 using C^1 quadratic isogeometric analysis with different quadrature rules.

Figure 5.6 shows the H^1-seminorm numerical errors of the eigenfunctions u_3 and u_{11} for C^1 quadratic isogeometric analysis with quadrature rules G_3, GL_3, G_2, and O_2. Their error convergence rate is two and the differences in the errors are fairly small. More precisely, Table 5.1 shows the errors for u_3. These numbers are the data for the left plot in Figure 5.6. Their differences are in the order of 10^{-6} for the case with mesh size 20 and of scale of 10^{-7} for the case with mesh size 40. As a

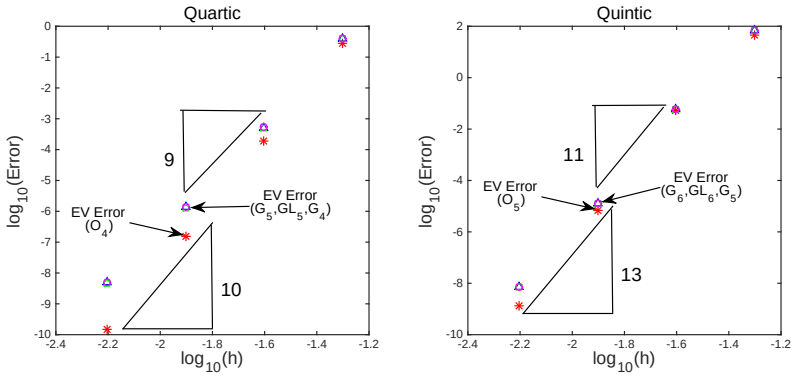

FIG. 5.5. *Dispersion errors for eigenvalue λ_{11} using quadrature rules G_5, GL_5, G_4, and O_4 for C^3 quartic isogeometric analysis (left) and G_6, GL_6, G_5, and O_5 for C^4 quintic isogeometric analysis (right).*

consequence, they have the same convergence rates. Similar results are observed for other eigenfunctions and details are omitted here.

For completeness, Figure 5.7 shows the eigenfunction errors in L^2-norm for C^1 quadratic case and Figure 5.8 for higher order cases. All the schemes yield errors which are of order $p+1$ for the p-th order isogeometric analysis of continuity C^{p-1}. These have the optimal convergence orders [7]. Again, the differences in errors when different quadrature rules are utilized are small.

Similar results are observed for C^2 cubic, C^3 quartic, and C^4 quintic isogeometric analysis (see Figure 5.8 for the quintic case). These numerical results confirm the eigenfunction error analysis in Section 4.2.

5.2. Convergence study in two dimension. The properties in two and higher dimensions are simple extensions of one dimensional cases when using tensor product meshes[15, 16]. Now, we consider the two-dimensional problem (2.2) with eigenvalues and eigenfunctions $\lambda_{jk} = \pi^2(j^2+k^2), u_{jk} = 2\sin(j\pi x)\sin(k\pi x), j,k = 1,2,\cdots$.

For more detailed numerical results in two dimension, we refer to [28]. We focus on convergence behavior of the method here. Figure 5.9 shows the dispersion errors for eigenvalue $\lambda_{2,2}$ using quadrature rules for C^1 quadratic, C^2 cubic, and C^3 quartic isogeometric elements. The mesh sizes for quadratic and cubic cases are $4\times4, 8\times8, 16\times16, 32\times32$, and 64×64, while the mesh sizes for quartic case are $4\times4, 8\times8, 16\times16$, and 32×32. We collect data for the coarser meshes since errors are of very small (up to machine precision) for the finer ones. The eigenvalue errors of the optimal blending schemes are of order $2p+2$, while the standard quadratures yield order $2p$. These observations verify the analysis we discussed above.

6. Concluding remarks. In this paper, we derive blending schemes to optimize the dispersion errors of isogeometric analysis. The dispersion error is minimized and smaller than the error obtained by optimally blended spectral-finite elements [3]; see [28] for a detailed comparison. Currently, the optimal blending schemes are established for p up to order seven for maximum continuity spaces. We will seek to generalize these results in the future work to arbitrary polynomial and continuity orders.

A topic that is not mentioned in this paper is the realization of the optimal blending schemes. At first glance, one needs to sample all the $p+1$ Gauss points

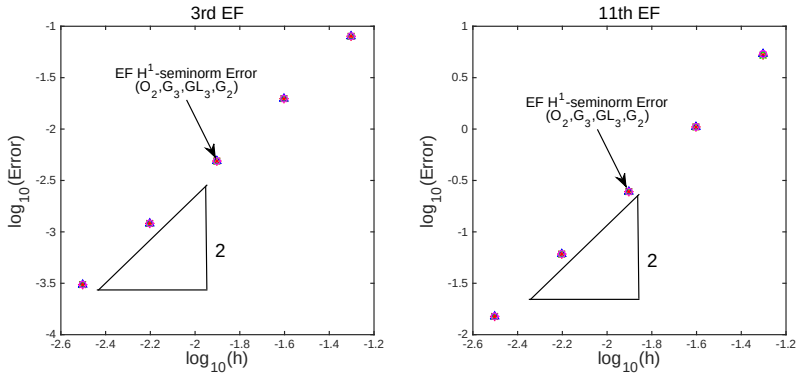

FIG. 5.6. *Eigenfunction H^1-seminorm errors for u_3 and u_{11} using C^1 quadratic isogeometric analysis with quadrature rules G_3, GL_3, G_2, and O_2.*

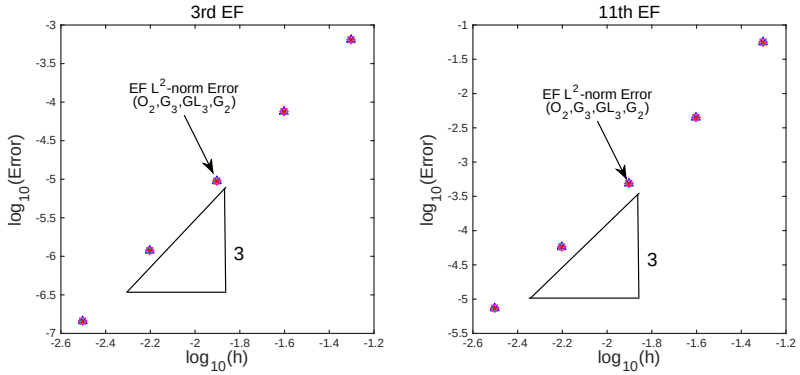

FIG. 5.7. *Eigenfunction L^2-norm errors for u_3 and u_{11} using C^1 quadratic isogeometric analysis with quadrature rules G_3, GL_3, G_2, and O_2.*

and $p+1$ Lobatto points for p-th order isogeometric analysis. This is not the case. Preliminary results show that a three-point non-standard quadrature rule is viable for C^2 cubic isogeometric elements. The number of points can be minimized following the work on optimal quadrature rules introduced in [6]. Further results in this direction will be reported in our future work.

7. Acknowledgments. This publication was made possible by the CSIRO Professorial Chair in Computational Geoscience of Curtin University, additional support was provided by the National Priorities Research Program grant 7-1482-1-278 from the Qatar National Research Fund (a member of The Qatar Foundation), and by the European Union's Horizon 2020 Research and Innovation Program of the Marie Skłodowska-Curie grant agreement No. 644202. The Spring 2016 Trimester on "Numerical methods for PDEs", organized with the collaboration of the Centre Emile Borel at the Institut Henri Poincare in Paris supported VMC's visit to IHP in October, 2016.

References.

[1] M. AINSWORTH, *Discrete dispersion relation for hp-version finite element approximation at high wave number*, SIAM Journal on Numerical Analysis, 42 (2004), pp. 553–575.

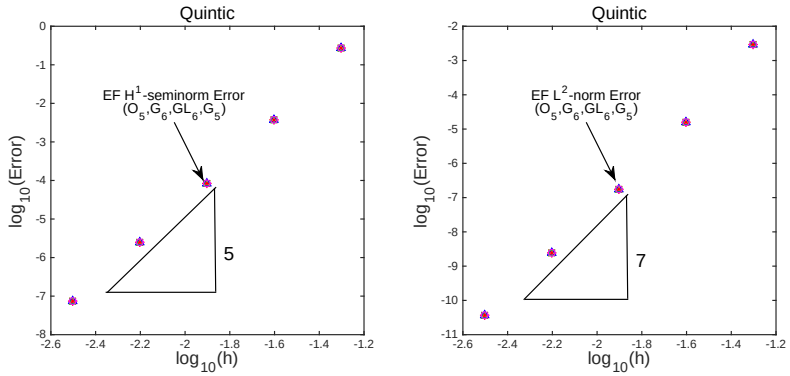

FIG. 5.8. *Eigenfunction H^1-seminorm (left) and L^2-norm (right) errors for u_{11} using C^4 quintic isogeometric analysis with quadrature rules G_6, GL_6, G_5, and O_5.*

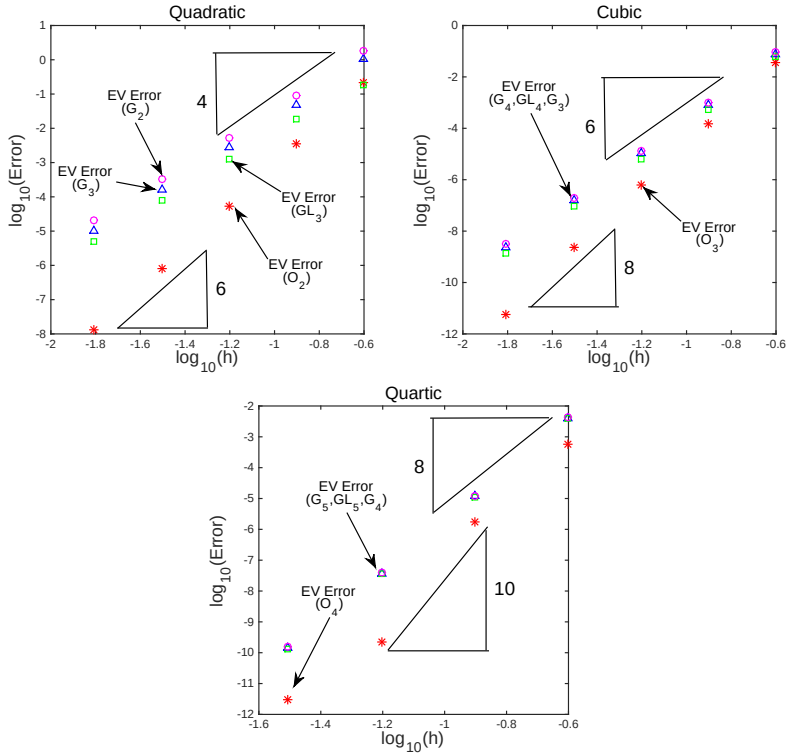

FIG. 5.9. *Dispersion errors for eigenvalue $\lambda_{2,2}$ using quadrature rules for C^1 quadratic, C^2 cubic, and C^3 quartic isogeometric analysis.*

[2] M. AINSWORTH AND H. A. WAJID, *Dispersive and dissipative behavior of the spectral element method*, SIAM Journal on Numerical Analysis, 47 (2009), pp. 3910–3937.

[3] ———, *Optimally blended spectral-finite element scheme for wave propagation and nonstandard reduced integration*, SIAM Journal on Numerical Analysis, 48 (2010), pp. 346–371.

[4] U. Banerjee, *A note on the effect of numerical quadrature in finite element eigenvalue approximation*, Numerische Mathematik, 61 (1992), pp. 145–152.
[5] U. Banerjee and J. E. Osborn, *Estimation of the effect of numerical integration in finite element eigenvalue approximation*, Numerische Mathematik, 56 (1989), pp. 735–762.
[6] M. Bartoň and V. M. Calo, *Optimal quadrature rules for odd-degree spline spaces and their application to tensor-product-based isogeometric analysis*, Computer Methods in Applied Mechanics and Engineering, 305 (2016), pp. 217–240.
[7] Y. Bazilevs, L. Beirao da Veiga, J. A. Cottrell, T. J. Hughes, and G. Sangalli, *Isogeometric analysis: approximation, stability and error estimates for h-refined meshes*, Mathematical Models and Methods in Applied Sciences, 16 (2006), pp. 1031–1090.
[8] V. A. Bokil, V. Gyrya, and D. A. McGregor, *A dispersion minimized mimetic method for cold plasma*, arXiv preprint arXiv:1604.01097, (2016).
[9] P. G. Ciarlet, *Finite Element Method for Elliptic Problems*, Society for Industrial and Applied Mathematics, Philadelphia, PA, USA, 2002.
[10] N. Collier, L. Dalcin, and V. M. Calo, *On the computational efficiency of isogeometric methods for smooth elliptic problems using direct solvers*, International Journal for Numerical Methods in Engineering, 100 (2014), pp. 620–632.
[11] N. Collier, L. Dalcin, D. Pardo, and V. M. Calo, *The cost of continuity: performance of iterative solvers on isogeometric finite elements*, SIAM Journal on Scientific Computing, 35 (2013), pp. A767–A784.
[12] N. Collier, D. Pardo, L. Dalcin, M. Paszynski, and V. M. Calo, *The cost of continuity: A study of the performance of isogeometric finite elements using direct solvers*, Computer Methods in Applied Mechanics and Engineering, 213 (2012), pp. 353–361.
[13] J. A. Cottrell, T. J. Hughes, and Y. Bazilevs, *Isogeometric analysis: toward integration of CAD and FEA*, John Wiley & Sons, 2009.
[14] J. A. Cottrell, A. Reali, Y. Bazilevs, and T. J. Hughes, *Isogeometric analysis of structural vibrations*, Computer methods in applied mechanics and engineering, 195 (2006), pp. 5257–5296.
[15] L. Gao, *Kronecker products on preconditioning*, PhD thesis, King Abdullah University of Science and Technology, 2013.
[16] L. Gao and V. M. Calo, *Fast isogeometric solvers for explicit dynamics*, Computer Methods in Applied Mechanics and Engineering, 274 (2014), pp. 19–41.
[17] M. N. Guddati and B. Yue, *Modified integration rules for reducing dispersion error in finite element methods*, Computer methods in applied mechanics and engineering, 193 (2004), pp. 275–287.
[18] I. Harari, *Reducing spurious dispersion, anisotropy and reflection in finite element analysis of time-harmonic acoustics*, Computer methods in applied mechanics and engineering, 140 (1997), pp. 39–58.
[19] I. Harari, M. Slavutin, and E. Turkel, *Analytical and numerical studies of a finite element PML for the Helmholtz equation*, Journal of Computational Acoustics, 8 (2000), pp. 121–137.
[20] Z. He, A. Cheng, G. Zhang, Z. Zhong, and G. Liu, *Dispersion error reduction for acoustic problems using the edge-based smoothed finite element method (ES-FEM)*, International journal for numerical methods in engineering, 86 (2011), pp. 1322–1338.
[21] T. J. Hughes, J. A. Cottrell, and Y. Bazilevs, *Isogeometric analysis:*

CAD, finite elements, NURBS, exact geometry and mesh refinement, Computer methods in applied mechanics and engineering, 194 (2005), pp. 4135–4195.

[22] T. J. Hughes, J. A. Evans, and A. Reali, *Finite element and NURBS approximations of eigenvalue, boundary-value, and initial-value problems*, Computer Methods in Applied Mechanics and Engineering, 272 (2014), pp. 290–320.

[23] T. J. Hughes, A. Reali, and G. Sangalli, *Duality and unified analysis of discrete approximations in structural dynamics and wave propagation: comparison of p-method finite elements with k-method NURBS*, Computer methods in applied mechanics and engineering, 197 (2008), pp. 4104–4124.

[24] F. Ihlenburg and I. Babuška, *Dispersion analysis and error estimation of Galerkin finite element methods for the Helmholtz equation*, International journal for numerical methods in engineering, 38 (1995), pp. 3745–3774.

[25] K. J. Marfurt, *Accuracy of finite-difference and finite-element modeling of the scalar and elastic wave equations*, Geophysics, 49 (1984), pp. 533–549.

[26] F. Odeh and J. B. Keller, *Partial differential equations with periodic coefficients and bloch waves in crystals*, Journal of Mathematical Physics, 5 (1964), pp. 1499–1504.

[27] D. Pardo, M. Paszynski, N. Collier, J. Alvarez, L. Dalcin, and V. M. Calo, *A survey on direct solvers for galerkin methods*, SeMA Journal, 57 (2012), pp. 107–134.

[28] V. Puzyrev, Q. Deng, and V. Calo, *Dispersion-optimized quadrature rules for isogeometric analysis: modified inner products, their dispersion properties, and optimally blended schemes*, arXiv preprint arXiv:1612.09097, (2017).

[29] S. I. Solovëv, *Approximation of differential eigenvalue problems*, Differential Equations, 49 (2013), pp. 908–916.

[30] S. I. Solovëv, *Finite element approximation with numerical integration for differential eigenvalue problems*, Applied Numerical Mathematics, 93 (2015), pp. 206–214.

[31] G. Strang and G. J. Fix, *An analysis of the finite element method*, vol. 212, Prentice-hall Englewood Cliffs, NJ, 1973.

[32] E. Süli, *Lecture notes on finite element methods for partial differential equations*, Mathematical Institute, University of Oxford, (2012).

[33] L. L. Thompson and P. M. Pinsky, *Complex wavenumber Fourier analysis of the p-version finite element method*, Computational Mechanics, 13 (1994), pp. 255–275.

[34] L. L. Thompson and P. M. Pinsky, *A Galerkin least-squares finite element method for the two-dimensional Helmholtz equation*, International Journal for numerical methods in engineering, 38 (1995), pp. 371–397.

[35] H. A. Wajid and S. Ayub, *An optimally blended finite-spectral element scheme with minimal dispersion for Maxwell equations*, Journal of Computational Physics, 231 (2012), pp. 8176–8187.